Available online at www.sciencedirect.com
SCIENCE DIRECT®
PHYSICS LETTERS B
ELSEVIER
Physics Letters B 555 (2003) 147–155
www.elsevier.com/locate/npe

ϕ production in Pb–Pb collisions at 158 GeV/c per nucleon incident momentum

NA50 Collaboration

B. Alessandro [k], C. Alexa [d], R. Arnaldi [k], J. Astruc [i], M. Atayan [m], C. Baglin [b], A. Baldit [c], S. Beolè [k], V. Boldea [d], P. Bordalo [g,1], G. Borges [g], A. Bussière [b], L. Capelli [l], V. Caponi [b], C. Castanier [c], J. Castor [c], B. Chaurand [j], I. Chevrot [c], B. Cheynis [l], E. Chiavassa [k], C. Cicalò [e], T. Claudino [g], M.P. Comets [i], N. Constans [j], S. Constantinescu [d], P. Cortese [a], J. Cruz [g], A. De Falco [e], N. De Marco [k], G. Dellacasa [a], A. Devaux [c], S. Dita [d], O. Drapier [j], L. Ducroux [l], B. Espagnon [c], J. Fargeix [c], P. Force [c], M. Gallio [k], Y.K. Gavrilov [h], C. Gerschel [i], P. Giubellino [k,2], M.B. Golubeva [h], M. Gonin [j], A.A. Grigorian [m], S. Grigoryan [m], J.Y. Grossiord [l], F.F. Guber [h], A. Guichard [l], H. Gulkanyan [m], R. Hakobyan [m], M. Idzik [k,3], D. Jouan [i], T.L. Karavitcheva [h], L. Kluberg [j], A.B. Kurepin [h], Y. Le Bornec [i], C. Lourenço [f], P. Macciotta [e], M. Mac Cormick [i], A. Marzari-Chiesa [k], M. Masera [k,2], A. Masoni [e], M. Monteno [k], A. Musso [k], P. Petiau [j], A. Piccotti [k], J.R. Pizzi [l], W. Prado da Silva [k,4], F. Prino [a], G. Puddu [e], C. Quintans [g], L. Ramello [a], S. Ramos [g,1], P. Rato Mendes [g], L. Riccati [k], A. Romana [j], H. Santos [g], P. Saturnini [c], E. Scalas [a], E. Scomparin [k], S. Serci [e], R. Shahoyan [g,5], F. Sigaudo [k], S. Silva [g], M. Sitta [a], P. Sonderegger [f,1], X. Tarrago [i], N.S. Topilskaya [h], G.L. Usai [e,2], E. Vercellin [k], L. Villatte [i], N. Willis [i]

[a] *Università del Piemonte Orientale, Alessandria and INFN-Torino, Italy*
[b] *LAPP, CNRS-IN2P3, Annecy-le-Vieux, France*
[c] *LPC, Univ. Blaise Pascal and CNRS-IN2P3, Aubière, France*
[d] *IFA, Bucharest, Romania*
[e] *Università di Cagliari/INFN, Cagliari, Italy*
[f] *CERN, Geneva, Switzerland*
[g] *LIP, Lisbon, Portugal*
[h] *INR, Moscow, Russia*
[i] *IPN, Univ. de Paris-Sud and CNRS-IN2P3, Orsay, France*
[j] *Laboratoire Leprince-Ringuet, Ecole Polytechnique and CNRS-IN2P3, Palaiseau, France*
[k] *Università di Torino/INFN, Torino, Italy*
[l] *IPN, Univ. Claude Bernard Lyon-I and CNRS-IN2P3, Villeurbanne, France*
[m] *YerPhI, Yerevan, Armenia*

Received 21 October 2002; received in revised form 18 December 2002; accepted 20 December 2002

Editor: L. Montanet

0370-2693/03/$ – see front matter
doi:10.1016/S0370-2693(02)03267-7

Abstract

The production of vector mesons ϕ, ρ and ω has been measured in Pb–Pb collisions at 158 GeV/c per nucleon incident momentum at the CERN/SPS. The muon spectrometer of experiment NA50 detects ϕ, ρ and ω mesons via their $\mu^+\mu^-$ decay channel in the collision center of mass rapidity range $0 \leqslant y_{\mathrm{CM}} \leqslant 1$. The results reported here show that the relative production of the ϕ compared to the $(\rho + \omega)$ and the ϕ multiplicity per participant nucleon (N_{part}) increase with the centrality of the collision. On the other hand, the $(\rho + \omega)$ multiplicity per participant does not exhibit any N_{part} dependence within our errors. The inverse slope parameter as deduced from an exponential fit to the ϕ transverse mass distribution is 228 ± 10 MeV. Our results are compared with those obtained by experiment NA49 and with theoretical calculations.

PACS: 25.75.Dw; 12.38.M; 14.40.Cs

Keywords: Quark–gluon plasma; Strangeness enhancement; Phi, rho and omega mesons

1. Introduction

Ultra-relativistic heavy ion collisions provide an experimental opportunity to study the properties of hadronic matter at high density and temperature. They can thus be used to probe the phase transition from ordinary matter to a deconfined quark–gluon plasma as theoretically predicted by QCD lattice calculations.

An enhancement of strange particle production has been predicted as a signature of such a transition [1], and extensively studied through strange meson and hyperon production [2,3]. In this context, the ϕ meson is of particular interest due to its $s\bar{s}$ valence quark content. Making use of their muon pair detection capabilities optimized for charmonium production [4,5], experiments NA38 and NA50 have extended their investigations to the lower part of the dimuon invariant mass spectrum and measured the features of ϕ, ρ and ω meson production in heavy ion collisions [6–8].

The ρ and ω vector mesons are combinations of $u\bar{u}$ and $d\bar{d}$ pairs and have masses close to the ϕ mass. This makes it particularly interesting to compare their production rate both as a function of their transverse mass and of the centrality of the collision.

Through the $\phi/(\rho + \omega)$ ratio we have access to the $s\bar{s}/(u\bar{u} + d\bar{d})$ ratio [9]. Due to its low interaction cross section, the ϕ meson could retain information of the critical phase of the collision during which the plasma proceeds to hadronization. Moreover, the identification of the vector mesons through their leptonic decay in the $(\mu^+\mu^-)$ channel should have some advantages as compared to their identification through hadronic decays (like the K^+K^- decay) as this latter sample could be affected by strong final state interactions [10].

Experiment NA38 has studied the ϕ and $\rho + \omega$ production in p–W, p–U, d–C, d–U, O–U, S–S, S–Cu and S–U collisions at 200 GeV/c per nucleon [6].

In this Letter, we report results obtained on Pb–Pb interactions at 158 GeV/c per nucleon incident momentum. They are based on a very large sample of events collected by the NA50 experiment during the run of 1996.

2. Experimental setup

A detailed description of the experimental setup can be found in [11]. Muon pairs from meson decays are detected in a spectrometer based on an air-gap toroidal magnet. The dimuon trigger makes use of the hits recorded by four scintillation counter hodoscopes which must include the pattern of 2 muon tracks originating from the target region and passing through all the elements of the spectrometer.

Events are selected in the collision center of mass rapidity window $0 \leqslant y_{\mathrm{CM}} \leqslant 1$ which lies inside the rapidity acceptance of the spectrometer. The muon

[1] Also at IST, Universidade Técnica de Lisboa, Lisbon, Portugal.
[2] Also at CERN, Geneva, Switzerland.
[3] Also at Faculty of Physics and Nuclear Techniques, Academy of Mining and Metallurgy, Cracow, Poland.
[4] Now at UERJ, Rio de Janeiro, Brazil.
[5] On leave of absence from YerPhI, Yerevan, Armenia.

angle defined in the Collins–Soper frame [12] is also restricted to the interval accepted by the spectrometer, namely, $-0.5 \leqslant \cos\theta_{\mathrm{C.S.}} \leqslant 0.5$. The NA50 spectrometer, as used for the study reported in this Letter, was kept in its standard configuration and, in fact, is optimized for the J/ψ meson detection. For lower mass resonances, its acceptance starts at a transverse mass of 1.5 GeV/c^2 and then rises up to values of 3% and 6.3%, respectively, for the ρ (ω) and for the ϕ meson, with these higher values reached for a transverse mass of 3 GeV/c^2.

The mass resolution, for these low mass muon pairs, is constant and results mainly from the multiple scattering of the muons passing through the spectrometer absorbers. It amounts to 70 MeV/c^2 and thus does not allow to separate the ω and ρ contributions. The results given in this Letter will, therefore, refer always to the sum $(\rho + \omega)$.

The centrality of the collision is estimated by an electromagnetic calorimeter which measures, on an event by event basis, the transverse energy (E_T) of the neutral particles produced in the collision, in the laboratory pseudo-rapidity interval $1.1 \leqslant \eta \leqslant 2.3$.

A very forward ("zero degree") hadronic calorimeter measures, for each Pb–Pb interaction, the energy of the non-interacting nucleons (spectators) of the Pb ion projectile. The same detector is used to trigger the apparatus on a sample of "minimum bias" events. This "minimum bias" trigger is completely independent from the dimuon trigger. It is obtained by requiring a non-zero energy deposit in the very forward calorimeter. It also requires a minimum value for the transverse energy recorded in the electromagnetic calorimeter in order to discard events which have not interacted in the target region.

The average beam intensity during data collection was 5.5×10^7 Pb ions per burst, with a spill of 4.5 s nominal duration. A total of 170 million events were recorded. Among them $\simeq 90\%$ were collected with the dimuon trigger and $\simeq 10\%$ with the minimum bias trigger. This led to ∼130 000 reconstructed ϕ mesons.

3. Data selection and analysis

Events are selected among a set of preselected runs satisfying standard conditions of beam quality and stability together with nominal operation conditions for every subdetector of the apparatus. Moreover, the surviving data are subject to a number of selection cuts in order to ensure that all the measured quantities are free from potential experimental biases. A detailed description of these selection criteria can be found in [4,11].

Fig. 1 displays a typical $\mu^+\mu^-$ invariant mass spectrum. The raw spectrum shows the resonant peaks corresponding to the ϕ, ρ and ω mesons, superimposed on a mass continuum. This mass continuum is made of correlated muon pairs arising from several physical processes, mainly Dalitz decays, $q\bar{q}$ annihilations and semileptonic decays of associated $D\overline{D}$ production. This "physical" continuum is mixed with a combinatorial background (called in short background from now on) which results from the abundant uncorrelated decays of mainly pions and kaons in the particular low mass range considered in this Letter. Because of their uncorrelation, these decays generate both opposite and like-sign muon pairs.

The background estimate is based on the "mirror" sample of like-sign muon pair events ($N^{\mu+\mu+}$ and $N^{\mu-\mu-}$) which are necessarily uncorrelated and which are collected, selected and reconstructed under conditions identical to the opposite-sign pairs.

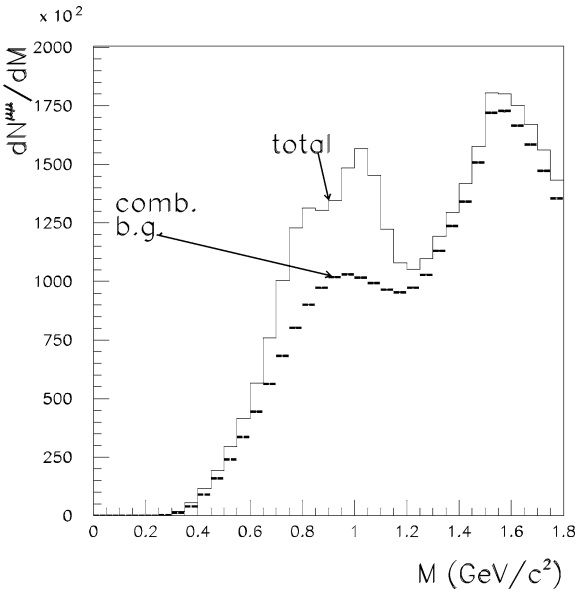

Fig. 1. Raw experimental mass spectrum ("total") of the detected $\mu^+\mu^-$ pairs with $M_T > 1.5$ GeV/c^2 for $E_T > 5$ GeV and combinatorial background ("comb. b.g.") mass spectrum.

The corresponding background muon pairs populating the opposite-sign invariant mass distribution have obviously the same properties and, in particular, the same shape as their reflected like-sign pairs, thanks to their identical acceptance resulting from an appropriate fiducial cut. It can be shown that they amount to $N_{\rm bg}^{\mu^+\mu^-} = 2 \times R \times \sqrt{N^{\mu^+\mu^+} N^{\mu^-\mu^-}}$. When non-correlation is perfectly satisfied, which is the case for high multiplicity Pb–Pb collisions, and when the different decay processes feeding the background have similar probabilities of producing a muon detected in the spectrometer, it can be further shown that $R = 1$ as both analytically computed [13] and confirmed through a Monte Carlo simulation [14]. Furthermore, when estimated without specific assumptions from a fit to our data sample, the same value $R \simeq 1$ is found [6] confirming, thereby, that the required conditions stated above are satisfied in our particular case. Numerically, the resulting uncorrelated background in the resonances mass range ($0.5 \leqslant M \leqslant 1.2$ GeV/c^2) amounts to 73% of the total muon pair yield.

In order to extract the number of ϕ, ρ and ω mesons from the dimuon mass spectra, we proceed as follows.

We make use of a complete simulation of the detector in order to account for the acceptance and smearing imposed by the apparatus to the decay muons produced in the collision. Each of the components of the mass spectrum is simulated according to production distributions depending on specific parameters which are adjusted, through an iterative procedure, by comparison with the actually collected data in the corresponding mass region, after background subtraction.

The ϕ and ω mass distributions are generated using Breit–Wigner shapes. For the ρ meson, a parametrization of the Breit–Wigner formula including a non-resonant background under the ρ, as in the HELIOS/3 experiment [15], is used. The transverse mass for the 3 resonances is generated according to the Hagedorn distribution, i.e., $dN/dM_T \propto M_T^2 K_1(M_T/T_p)$ [16] where K_1 is a Bessel function and T_p a parameter. The rapidity is generated according to a Gaussian distribution (centered at mid-rapidity). The continuum is treated in a phenomenological way according to $dN/dM \propto 1/M^{\alpha} e^{-M/\beta}$. Its transverse mass and rapidity distributions are taken with the same analytical shapes as adopted for the resonances. The parameters of these generation functions (T_p, the rapidity distribution width, α and β parameters of the continuum) are adjusted on the experimental distributions separately for each component as defined by its corresponding mass region.

With the generation functions of each of the components determined as described above, we generate and reconstruct each of the components of the mass spectrum and describe the shape of the detected muon pairs as seen by the detector. We then fit, after subtraction of the combinatorial background, the experimental dimuon mass spectra between 0.25 and 1.8 GeV/c^2 to the following expression:

$$\frac{dN^{\mu^+\mu^-}}{dM} = A_{\rho+\omega}\big[F_\rho(M) + R_{\rm Br} F_\omega(M)\big] + A_\phi F_\phi(M) + A_{\rm CNT} F_{\rm CNT}(M), \qquad (1)$$

where the F functions are the mass distributions corresponding to each of the components "as seen" by the detector. Fig. 2 shows the dimuon invariant mass spectrum superimposed to the fitting function. The F_ω and F_ϕ functions are Gaussian and reproduce

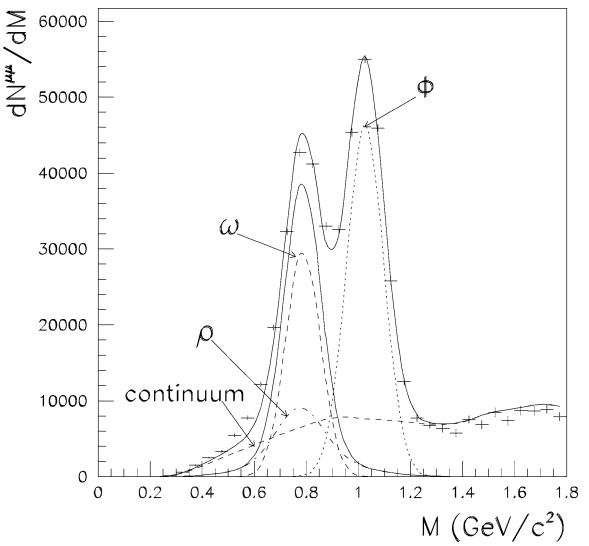

Fig. 2. Fit of the spectrum of the $\mu^+\mu^-$ pairs (combinatorial background subtracted) with $M_T > 1.5$ GeV/c^2 for $E_T > 5$ GeV.

[6] This has been checked by fitting the muon pair invariant mass distribution in the mass range 1.6–2.5 GeV/c^2, assumed as made of Drell–Yan pairs, semi-leptonic decays of associated $D\overline{D}$ production and uncorrelated background shaped by the corresponding like-sign pairs. When leaving as free parameters the amount of each component, the fitted value of R is 1.015 ± 0.08.

with good accuracy the resolution of the detector as determined by Monte Carlo simulation. There are 5 free parameters in the fit: the three amplitudes ($A_{\rho+\omega}$, A_ϕ and A_{CNT}) and the center position of the two Gaussians (F_ω and F_ϕ). The same cross section was assumed for ρ and ω production (as observed in p–p collisions at 400 GeV/c [17]), so that the amplitude $A_{\rho+\omega}$ is the same for the two resonances. R_{Br} takes into account the difference between the ρ and ω branching ratios into $\mu^+\mu^-$. The numbers of ϕ, ρ and ω in the nine transverse energy (E_T) bins and the five dimuon transverse mass (M_T) bins considered in this study are finally extracted using exactly the same procedure.

The continuum is adjusted on the mass spectrum below and over the $\rho+\omega$ and ϕ peaks by an ad-hoc 2 parameter function. It is then interpolated in the resonance mass region by a smooth variation of the parameters. The procedure is the same in each transverse mass bin.

It is worthwhile underlining here that if the combinatorial background is subtracted in a different way, namely, with a different value of R, the function to which the continuum is adjusted is then different. Nevertheless, the resonance peaks remain the same, provided that the combinatorial background is a smooth function of the mass and does not display any peak under the resonances. This is definitely the case from the experimental shape as determined from the combinatorial like-sign mass spectrum. Therefore, the numbers of ϕ, ρ and ω mesons determined by this method are not sensitive to the absolute value of R.

The uncertainty of the method on the acceptances as well as on all the results which are presented hereafter is carefully determined by slightly varying the generation parameters [8].

4. Results

The ratio $(\phi/(\rho+\omega))_{\mu\mu}$ of the produced ϕ and $\rho+\omega$ resonances decaying into a $\mu^+\mu^-$ pair, already corrected for acceptance, is shown in Fig. 3 as a function of the transverse mass for the whole E_T domain ($E_T > 5$ GeV). This quantity is independent of the trigger and reconstruction efficiencies which cancel out in the ratio. The smaller error bars in Fig. 3 correspond to the statistical and to the fit uncertainties.

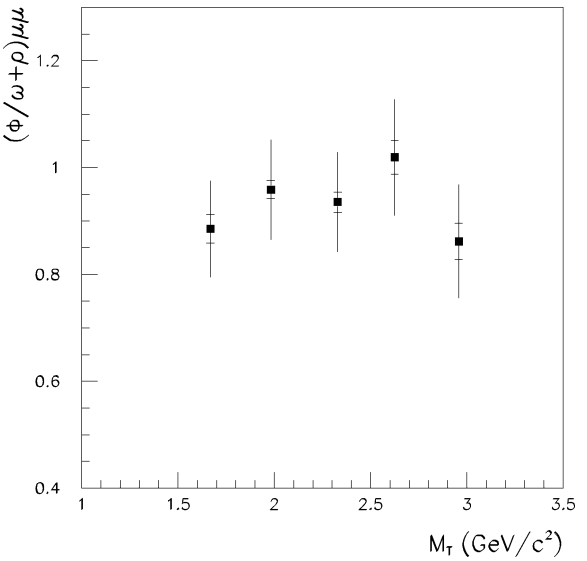

Fig. 3. The ratio $(\phi/(\rho+\omega))_{\mu\mu}$ of the number of produced ϕ and $\rho+\omega$ mesons and decaying into a $\mu^+\mu^-$ pair, as a function of the dimuon transverse mass (M_T) over the whole E_T domain ($E_T > 5$ GeV).

The larger error bars include, added in quadrature, the method uncertainty which depends on M_T. As can be seen from the figure, the general trend is flat, which indicates that the ϕ and $\rho+\omega$ production rates have similar M_T dependences.

The same ratio is presented in Fig. 4 as a function of the number of participant nucleons, for the whole M_T domain, namely $M_T \geqslant 1.5$ GeV/c^2. The number of participant nucleons (N_{part}) is deduced for each E_T bin from the mean E_T value, using the Glauber and the wounded nucleon models [18–20]. Again the error bars correspond to the statistical and to the fit uncertainties. A 9.5% method uncertainty should be added in quadrature, but it affects all the points coherently and thus should be disregarded when considering only the trend of the N_{part} dependence. The $(\phi/(\rho+\omega))_{\mu\mu}$ ratio exhibits a 70% increase when going from the most peripheral to the most central collisions and flattens for $N_{\mathrm{part}} \geqslant 250$. The same behavior is observed for each M_T bin.

ϕ and $(\rho+\omega)$ multiplicities are measured for the first time in the NA50 experiment. They allow in particular to check that this increase comes from an enhancement of the ϕ production. The ϕ meson multiplicity is the number of ϕ mesons produced per

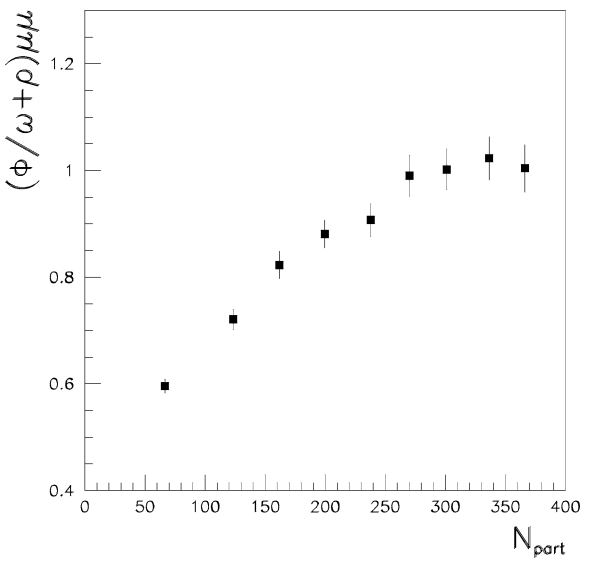

Fig. 4. The ratio $(\phi/(\rho+\omega))_{\mu\mu}$ as a function of the number of participant nucleons (N_{part}) over the whole $M_T \geqslant 1.5$ GeV/c^2 domain.

Pb–Pb collision. It is calculated from the ratio of the number of measured ϕ mesons, N_ϕ^{meas}, corrected for acceptance (Acc_ϕ), trigger ($\varepsilon_{\text{trig}}$) and reconstruction ($\varepsilon_{\text{rec}}$) efficiencies, to the number of minimum bias Pb–Pb collisions:

$$\Delta N_\phi^{\mu\mu} = N_\phi^{\mu\mu}(\Delta E_T) = \frac{N_\phi^{\text{meas}}(\Delta E_T)/Acc_\phi}{N_{\text{M.B.}}(\Delta E_T) \times \varepsilon_{\text{trig}} \times \varepsilon_{\text{rec}}}.$$

On the left-hand side of Fig. 5, are shown the ϕ and $\rho+\omega$ multiplicities in the $\mu^+\mu^-$ channel vs. the number of participant nucleons. The error bars correspond to the statistical and the fit uncertainties. A method uncertainty—of 8.6% for the ϕ meson and 5.4% for $\rho+\omega$ mesons—and a 2.3% systematic uncertainty should be added respectively in quadrature and linearly. As these errors affect all the points coherently, they should be disregarded when considering only the trend of the N_{part} dependence. The multiplicities increase as N_{part} increases. To further quantify this increase, the multiplicities are divided by the number of

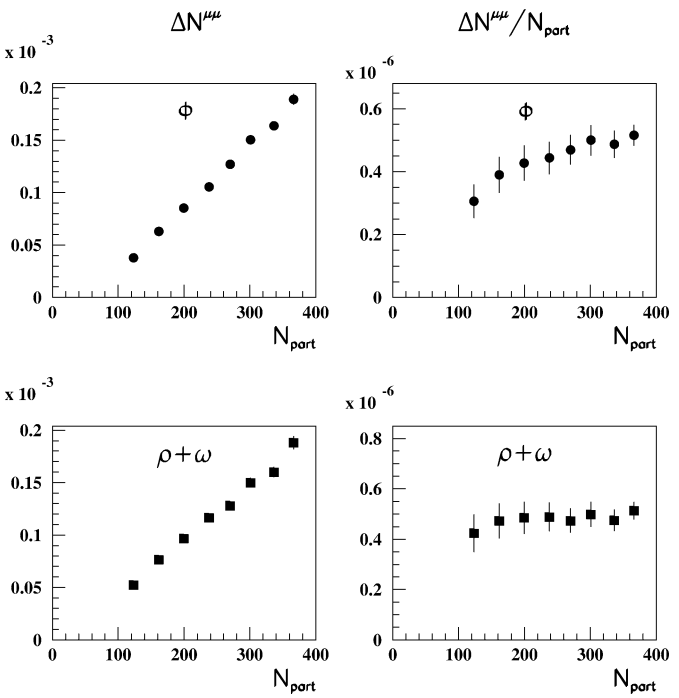

Fig. 5. Multiplicities (left panels) and multiplicities per participant nucleon (right panels), corrected for acceptance, for the ϕ and $\rho+\omega$ mesons with $M_T > 1.5$ GeV/c^2. (The background being different in a minimum bias event and in a dimuon event, the first point has been omitted here due to the contamination from Pb–air interactions in the minimum bias sample.)

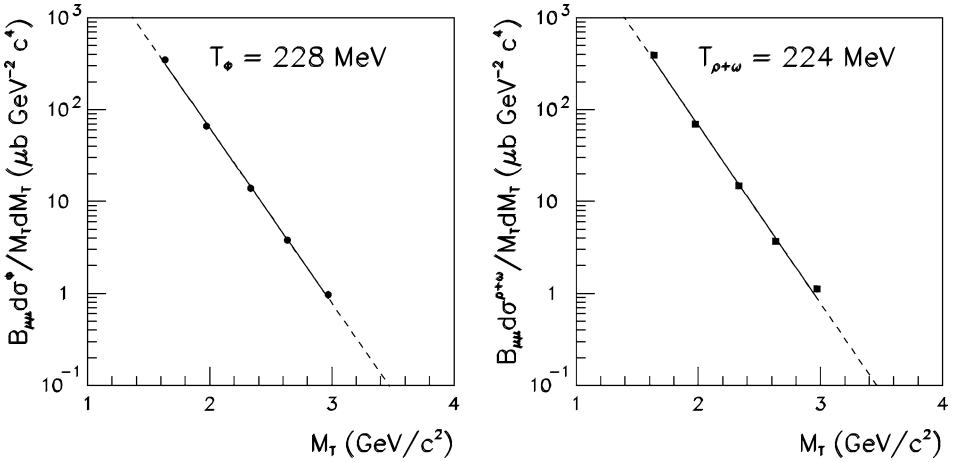

Fig. 6. Fit of the cross-section distributions vs. M_T for ϕ and $\rho+\omega$, for the whole E_T domain.

Table 1
Effective temperature values for the ϕ and $\rho+\omega$ mesons for each transverse energy bin (E_T)

ΔE_T (GeV)	5–29	29–42	42–53	53–64	64–74	74–83	83–93	93–105	>105
T^ϕ (MeV)	218 ± 6	229 ± 7	225 ± 7	225 ± 7	231 ± 7	229 ± 6	229 ± 6	231 ± 8	234 ± 7
$T^{\rho+\omega}$ (MeV)	221 ± 4	221 ± 5	224 ± 5	223 ± 7	230 ± 6	223 ± 6	225 ± 7	232 ± 7	221 ± 6

participant nucleons, and plotted vs. N_{part}, as shown on the right side of Fig. 5. The additional N_{part} uncertainty, given by the half FWHM of the N_{part} distribution in the corresponding centrality bin, has been introduced in the figure. Within our errors, one can observe a flat behavior for the $\rho+\omega$ multiplicity when normalized by N_{part}, while there is an increase of ~ 1.7 of the ϕ multiplicity which seems to flatten beyond $N_{\text{part}} \simeq 250$. This increase of the ϕ meson multiplicity divided by N_{part} is observed in each of the five M_T bins.

The ϕ and $\rho+\omega$ production cross sections have been measured through the dimuon decay channel ($B_{\mu\mu} \times \sigma^{\phi,\rho+\omega}$). The $B_{\mu\mu} \times d\sigma^{\phi,\rho+\omega}/M_T\, dM_T$ quantities are plotted vs. M_T on Fig. 6, for the whole E_T domain. The error bars include the statistical, the fit and the method errors. A systematic uncertainty of 6.9% has to be added linearly. We choose to fit the $B_{\mu\mu} \times d\sigma^{\phi,\rho+\omega}/M_T\, dM_T$ spectra with $M_T e^{-M_T/T}$, as used by other experiments, which leads to the inverse slope parameters $T_\phi \simeq 228 \pm 10$ MeV and $T_{\rho+\omega} \simeq 224 \pm 10$ MeV within the studied M_T range. When the same analysis is repeated in each E_T bin, the effective temperatures are found to be independent of the centrality as can be seen in Table 1.

5. Discussion and conclusions

As previously observed in the NA38 experiment in S–S, S–Cu and S–U interactions [6], the $(\phi/(\rho+\omega))_{\mu\mu}$ ratio increases with increasing centrality in Pb–Pb reactions. The large data sample collected in 1996 for Pb–Pb collisions allows us to observe a saturation effect of this ratio for N_{part} greater than 250. The ϕ meson multiplicity per participant nucleon seems to display the same behavior.

This pattern is different from the one measured by the WA97 experiment for multi-strange baryons for which production yields saturate at around $N_{\text{part}} \simeq 100$ [3].

On the other hand, the ratio $(\phi/(\rho+\omega))_{\mu\mu}$ and the ϕ meson multiplicity pattern display the same behavior as the ϕ/π and K/π ratios measured by the NA49 Collaboration [2,21], as well as the K/π ratio at lower energies (at the AGS in the E866 experiment [22]).

The ϕ effective temperature we obtain is very different from the value obtained by the NA49 experiment which, moreover, varies slightly with centrality [2]. For the most central collisions, representing

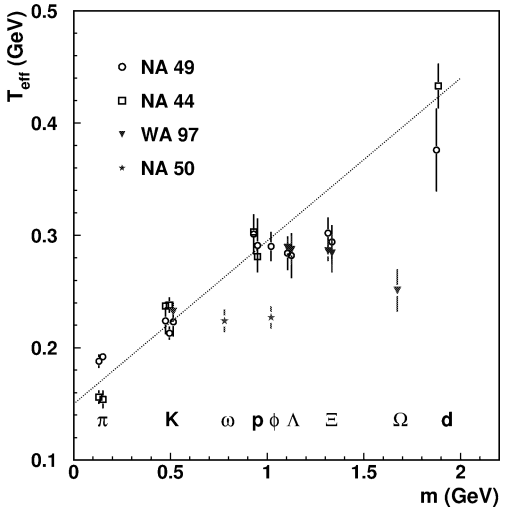

Fig. 7. Effective temperatures vs. particle mass measured by several experiments in Pb–Pb collisions at 158 GeV/c per nucleon at the CERN/SPS.

5% of the total cross section, the effective temperature measured by the NA49 experiment is 305 ± 15 MeV, whereas we obtain 230 ± 10 MeV. The M_T domains covered by the two experiments are different, but even in the common M_T range (1.5–2.4 GeV/c^2) the NA50 invariant slope 216 ± 15 MeV remains lower than the NA49 one $\simeq 290$ MeV. It is also clear that the two experiments do not measure the ϕ resonance through the same decay channel, but this does not seem enough to explain the discrepancy [10].

The effective temperature provides information on the collective transverse flow and the conditions of the system at the moment when the particles under study cease interacting elastically. This is usually described by 2 parameters, namely, the thermal freeze-out temperature $T_{\rm th}^{\rm fo}$, and the mean velocity of the transverse collective flow v_T [23]. For low momenta, $T_{\rm eff}$ is expected to increase linearly with the particle mass: $T_{\rm eff} \simeq T_{\rm th}^{\rm fo} + 1/2 m v_T^2$. In Fig. 7 are plotted the effective temperatures $T_{\rm eff}$ vs. the mass of the particules as measured in Pb–Pb collisions by several experiments at the CERN/SPS, although not in the same M_T range. The $T_{\rm eff}$ values corresponding to non-strange and single-strange hadrons are well reproduced by the straight line deduced from RQMD calculations [24]. The Ω and $\overline{\Omega}$ effective temperature obtained by the WA97 experiment [25] is clearly below the line. The ϕ meson effective temperature extracted from our measurement is also below the line, even if we take into account the local slope variation of ± 25 MeV on our M_T range. The Ω and $\overline{\Omega}$ (anti)baryons, being composed of strange quarks (or antiquarks) only, have smaller interaction cross sections in the hadron gas as compared to other hadrons. These particles should decouple earlier from the hadron gas, and therefore be less affected by the transverse collective flow, which would explain their low effective temperature [24]. The same scenario could apply to the ϕ meson. This idea is supported by the fact that the MICOR model [26], in which there are no interactions in the hadron gas, reproduces the ϕ, Ω and $\overline{\Omega}$, as well as the $\rho + \omega$ effective temperatures.

References

[1] B. Muller, J. Rafelski, Phys. Rev. Lett. 81 (1986) 1066.
[2] S.V. Afanasiev, et al., NA49 Collaboration, Phys. Lett. B 491 (2000) 59;
S.V. Afanasiev, et al., Nucl. Phys. A 698 (2002) 104c.
[3] F. Antinori, et al., WA97 Collaboration, Nucl. Phys. A 661 (1999) 130c.
[4] M.C. Abreu, et al., NA50 Collaboration, Phys. Lett. B 450 (1999) 456.
[5] M.C. Abreu, et al., NA50 Collaboration, Phys. Lett. B 477 (2000) 28.
[6] C. Baglin, et al., NA50 Collaboration, Phys. Lett. B 272 (1991) 449;
M.C. Abreu, et al., Phys. Lett. B 368 (1996) 239;
J. Astruc, Ph.D. Thesis, Université Paris 6—Pierre et Marie Curie, 1997;
C. Quintans for the NA50 Collaboration, J. Phys. G: Nucl. Part. Phys. 27 (2001) 405.
[7] N. Willis for the NA50 Collaboration, Nucl. Phys. A 661 (1999) 534;
M.P. Comets for the NA50 Collaboration, Nucl. Phys. A 663–664 (2000) 721c;
L. Villatte for the NA50 Collaboration, XXXVIII International Winter Meeting on Nuclear Physics, Bormio, Italy, supplemento No. 116 (2000) 241.
[8] L. Villatte, Ph.D. Thesis, Université Paris 7—Denis Diderot, 2001.
[9] A. Shor, Phys. Lett. 54 (1985) 1122.
[10] S.C. Johnson, B.V. Jacak, A. Drees, Eur. Phys. J. C 18 (2001) 645;
S. Soff, et al., J. Phys. G: Nucl. Part. Phys. 27 (2001) 449.
[11] M.C. Abreu, et al., NA50 Collaboration, Phys. Lett. B 410 (1997) 327.
[12] J.C. Collins, D.E. Soper, Phys. Rev. D 16 (1977) 2219.
[13] S. Papillon, Ph.D. Thesis, Université Paris-Sud, 1993.
[14] M.C. Abreu, et al., NA50 Collaboration, Euro. Phys. J. C 14 (2000) 443;

C. Soave, Ph.D. Thesis, Università degli Studi di Torino, 1998.
[15] A. Angelis, et al., HELIOS3 Collaboration, Eur. Phys. J. C 5 (1998) 63.
[16] R. Hagedorn, Rivista Nuovo Cimento 6 (1983) 10.
[17] M. Aguilar-Benitez, et al., LEBC-EHS Collaboration, Z. Phys. C 50 (1991) 405.
[18] R.J. Glauber, High Energy Collision Theory, in: Lectures in Theoretical Physics, Vol. I, Interscience, New York, 1959, p. 315.
[19] A. Bialas, M. Bleszyński, W. Czyz, Nucl. Phys. B 111 (1976) 461.
[20] D. Kharzeev, C. Lourenço, M. Nardi, H. Satz, Z. Phys. C 74 (1997) 307.
[21] C. Höhne for the NA49 Collaboration, Nucl. Phys. A 661 (1999) 485c.
[22] C.A. Ogilvie for the E866 and E917 Collaborations, Nucl. Phys. A 638 (1998) 57c.
[23] N. Xu for the NA44 Collaboration, Nucl. Phys. A 610 (1996) 175c.
[24] H. van Hecke, H. Sorge, N. Xu, Phys. Rev. Lett. 81 (1998) 5764.
[25] F. Antinori, et al., WA97 Collaboration, Eur. Phys. J. C 14 (2000) 633.
[26] P. Csizmadia, P. Levai, Phys. Rev. C 61 (2000) 031903(R).